

# Data Analysis & Handling Project 5

## Studies of $B^+ \rightarrow J/\psi K^+$

Waiton, John  
[s1739002@ed.ac.uk](mailto:s1739002@ed.ac.uk)  
University of Edinburgh  
School of Physics and Astronomy

### Abstract

The goal of this project is to study LHCb data of the decay  $B^+ \rightarrow J/\psi K^+$ , and ascertain values for the masses & yields of the  $B^\pm$  mesons, as well as investigate the lifetime of said mesons. This will be achieved using python code that allows us to analyse the data, using side-band subtraction & maximum likelihood fitting to find the appropriate values that describe our data's resulting Mass, Yield and Lifetime.

# 1 Introduction

## 1.1 Background

The data that will be analysed in this report comes from a 2017 paper [1] on the mesons  $B^\pm(u\bar{b}/\bar{u}b)$ ,  $J/\psi(c\bar{c})$  and  $K^+(u\bar{s})$  in the decay  $B^+ \rightarrow J/\psi K^+$ . The data was collected by the LHCb experiment while it was running, which focused its attention on experimentation relating to b-physics<sup>1</sup>, via 6 key measurements fully described in their roadmap [2].

The 2017 paper that our data is sourced from was on the production cross-section of  $B^\pm$  mesons in  $pp$  collisions, as the experiment acted as a test for certain theoretical quantum chromodynamic calculations (FONLL<sup>2</sup>) [3], with the paper concluding that the results agreed with said calculations.

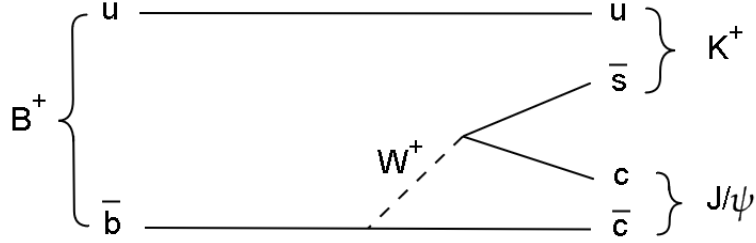


Figure 1: A feynmann diagram of the  $B^+ \rightarrow J/\psi K^+$  decay [4]

## 1.2 Aim

The main topics of focus in this project will be the invariant mass distribution of this decay, and the lifetime of the  $B^\pm$  mesons in the decay. Using python, the data provided will be represented in the forms of histograms, that allows us to more easily understand the distributions of the  $B^\pm$  meson's invariant masses and lifetimes. We will then use side-band subtraction and maximum likelihood fitting to find values for the Yield, Mean Mass & Lifetime of the  $B^\pm$  mesons. This will be done via the use of python, and throughout the report each section will have more detail of how exactly this is achieved.

---

<sup>1</sup>Physics relating to the bottom quark

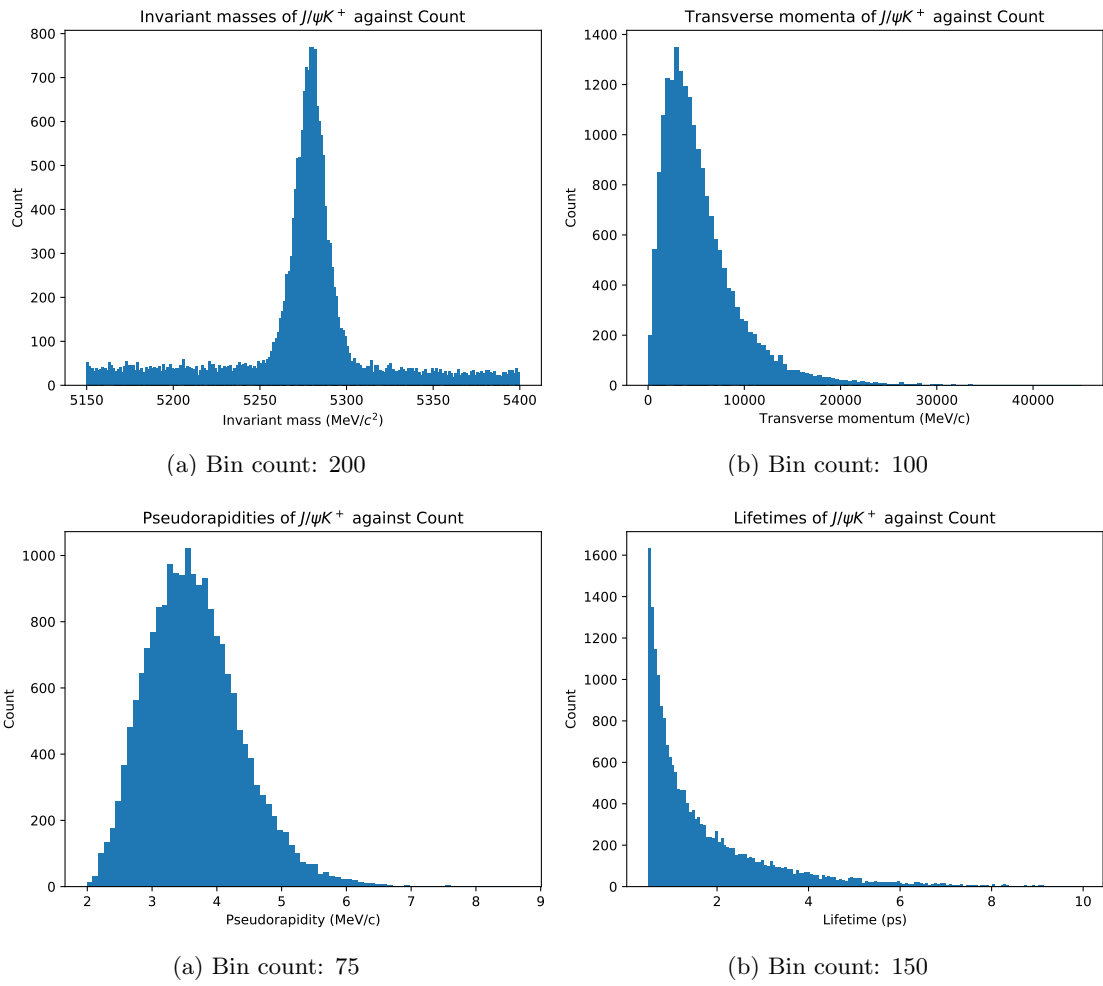
<sup>2</sup>(fixed-to-next-to-the-leading order)

## 2 Histograms and Peak Finding

### 2.1 Histograms

The majority of our analysis will be pertaining to the smaller data sample (kdata-small.bin), which we will plot and study with the use of histograms. To analyse this sufficiently, the number of bins for each component of our sample had to be determined. This was to ensure that the bins weren't too small so that the trends of our data could be ascertained, without creating too much uncertainty via oversized bins.

The five components of our data sample were the invariant mass, transverse momentum, pseudo-rapidity, charge and lifetimes of the  $J/\psi K^+$  candidates. For each, the bins had to be fine-tuned to get results that meet our previously stated expectations.



The histogram for the charge needs to be considered separately, as the charges are exclusively found to be  $\pm 1$ . Histograms have difficulty expressing this as getting a bin size that would cover **only**  $\pm 1.0$  would require  $\infty$  bins, as the bin width decreases with the number of bins. This is important to keep in mind when looking at the resulting histogram.

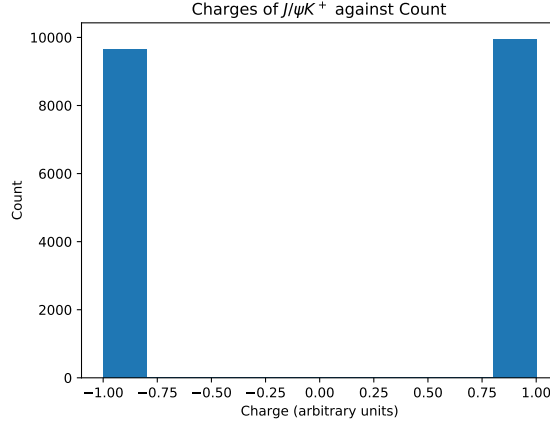
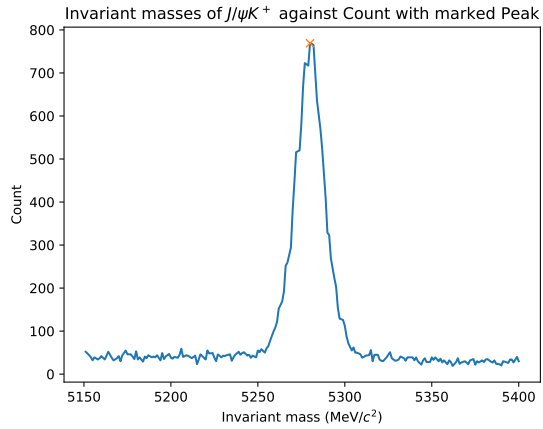


Figure 4:

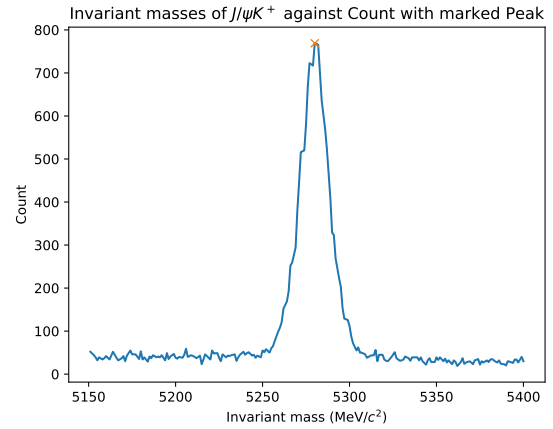
Bin Count: 10 - Chosen just for clarity of the two separate peaks, no information is gained or lost from choosing a different bin size.

## 2.2 Peak Finding

From this, we will mostly focus on the invariant mass component of our acquired data. We initially are trying to find the peak of our mass-count graph to determine a good estimate value for our  $B^\pm$  meson mass. Within our python code, the function `find_peaks`, from the `scipy` library [5] was used to determine exactly which bin had the highest number of entries in the peak region. This method was tested with both 200 and 300 bins to determine if the difference was significant;



(a) Bin count: 200 - X marks the peak.



(b) Bin count: 300 - X marks the peak.

For these peak values, the bin centers were determined to be  $5279.355(625) \text{ MeV}/c^2$  and  $5279.56(42) \text{ MeV}/c^2$  respectively. This was determined by taking the mean of the bin edges to find the value, and taking the uncertainty to be half the bin width. As can be seen in these results, the difference between 200 and 300 bins is negligible, and both values fall within their respective uncertainty values.

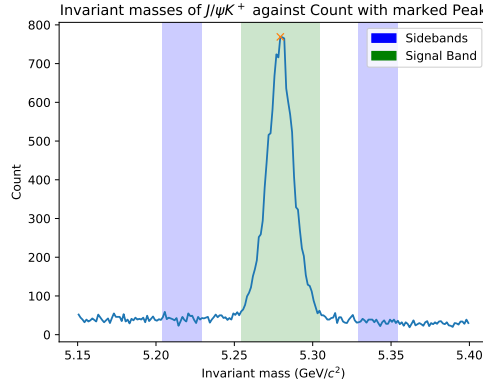
Comparing our estimation to the literature value of  $5279.34(12) \text{ MeV}/c^2$  [6], we find the estimate value to be well within  $1\sigma$ , but with a much larger uncertainty due to the source of the uncertainty being the bin size. This demonstrates the issue with this method of estimation, as our uncertainty can be reduced with more rigorous statistical analysis.

Assuming that the shape of our mass distribution is Gaussian, we can estimate a value for the Full Width Half Maximum (FWHM) and resolution of our  $B^\pm$  meson mass distribution. Our bin with the highest count was found to have 769 events within it. Our FWHM can then be found by determining the binned mass values on each side of the distribution that contain approximately 384.5 events. These were found to be  $5270.04$  &  $5288.75 \text{ MeV}/c^2$  respectively. This allows us to determine the FWHM to be approximately  $18.71 \text{ MeV}/c^2$ , allowing us to determine a resolution value for the distribution, using  $FWHM = 2\sigma\sqrt{2\ln 2}$ . The resolution was found to be  $7.9412 \text{ MeV}/c^2$ . This is significantly larger than the uncertainty found previously, but is flawed due to the assumption of a Gaussian shape for our data sample.

Due to issues in the code, from this point onward all graphs related to the mass will be referred to in  $\text{GeV}/c^2$ . This is due to technical limitations in Python, as overflow errors would occur if  $5000 \text{ MeV}/c^2$  was applied within an exponential, but not  $5 \text{ GeV}/c^2$ . While this is the case in the code and graphs, when comparing to literature values,  $\text{MeV}/c^2$  will be used for clarity, as  $\text{MeV}/c^2$  is the standard unit in most papers on  $B^\pm$  meson decay.

### 3 Side-bands and Signal Region

To collect an estimate for the number of 'signal'<sup>3</sup> events, a signal region had to be decided, and was determined to be  $\pm 25 \text{ MeV}/c^2$  around the peak value, with our background side-bands being half the size of this region, and equidistant from it on both sides. Assuming that the background is linear across mass, determining the number of events in these separate regions allows us to eliminate the background events from the signal region, giving us a reasonable value for the yield of  $B^\pm$  mesons in the signal region. This was done within our code and is known as 'side-band subtraction'



The reduced signal region was found to have 12010 events within it, giving us a reasonable value for our  $B^\pm$ 's yield. The errors on this value are hard to quantify, as the signal region choice was arbitrary as was the distance of the side-bands from the signal band. The background events are expected to decrease linearly with mass, so there are possible issues with determining the value for yield this way, but investigating this aspect of the analysis further goes beyond the scope (& time limitations) of this project.

<sup>3</sup>Events that described the  $B^\pm$  mesons, rather than background noise.

## 4 Composite Probability Density Function and Fitting

### 4.1 Method - Composite PDF and Negative Log Likelihood

To obtain a better result for our mean mass value, a composite PDF was determined considering the separate components of our  $B^\pm$  distribution:

- A Gaussian PDF for the central mass peak.
- An exponential PDF for the background events.

The composite PDF must be normalised, to ensure this, both were kept as ratios to one another totalling in a value of 1;

$$PDF = (1 - F) \cdot (PDF_{Exponential}) + (F) \cdot (PDF_{Gaussian}) \quad (1)$$

The exponential and Gaussian PDFs were then normalised. The Gaussian PDF was normalised across all of space ( $\pm\infty$ ) as its values become negligible beyond the peak, but our Exponential PDF had to be normalised across the mass range, as its components outwith the considered mass range were still significant enough to affect our results.

$$PDF_{norm} = (1 - F) \cdot \left( \frac{\lambda}{e^{-x_{min}} - e^{-x_{max}}} \right) \cdot (e^{-\lambda x}) + (F) \cdot \left( \frac{1}{\sqrt{2\pi}\sigma} \right) \cdot (e^{-\frac{1}{2}(\frac{x-\mu}{\sigma})^2}) \quad (2)$$

The function `curve_fit` [7] was utilised to find optimal parameters for fitting our PDF to the initial unbinned data. The optimal parameters were used in our maximum likelihood fit, in which the negative log likelihood of our PDF was minimised using `scipy.optimize.minimize` [8]. The 'Nelder-Mead' minimisation method was chosen. The negative log likelihood function was derived as shown:

$$NLL = - \sum \log(PDF_{norm}) \quad (3)$$

The minimize function was allowed to vary all values of  $\lambda, F, \mu$  and  $\sigma$  with the initial unbinned data, to minimise the NLL function. This found the most appropriate fit for our data, which could then be used to determine the mass value of our  $B^\pm$  mesons, as well as giving another estimate for our yield. An issue with using the Nelder-Mead method was that it doesn't give any errors on the parameters it minimises. Methods that do return these errors would not successfully minimise the function, and so a different method for finding these parameter errors had to be found.

The method used to determine the parameter errors was quite simple, the chosen parameter was held fixed at a value a small increment off its minimised value, and the minimisation engine was run again. The new negative log likelihood function value was found, and if it was  $\pm 0.5$  from the initial NLL minimised value, then the difference in our fixed parameter when compared to the initial parameter was the parameter error. If the NLL value was less than  $\pm 0.5$ , then the fixed value was increased/decreased again by a small increment and the process was repeated. The increments taken must be **smaller** than the parameter value, such that the error found isn't significantly affected by the size of the increments taken. Due to the computational requirements for the parameter error finding process, the parameter error for  $\mu$  was the only ones found, as it was considered the most relevant error for our project.

### 4.2 Maximum Likelihood Fit Results

Applying our previously described method to our  $B^\pm$  data, the parameters  $F, \mu, \sigma$ , &  $\lambda$  were found to be:

	F (-)	$\mu$ ( $GeV/c^2$ )	$\lambda$ (-)	$\sigma$ ( $GeV/c^2$ )
Value	0.6164	5.279305	1.446012	8.97663e-03
Error	-	9.5e-05	-	-

The  $\sigma$  value is two orders of magnitude larger than the  $\mu$  parameter error. This implies that there are sources of uncertainty not considered within our method, and that our parameter error is not a good representation of our  $\mu$  uncertainty. From this point onwards, the parameter error for  $\mu$  will be disregarded in the  $\mu$  uncertainty, but will still be calculated for completeness.

For our values of yield, it is assumed that the Gaussian PDF accounts for all  $B^\pm$  mesons, and so the F value corresponding to the Gaussian-Exponential PDF ratio can be multiplied with the number of total events (19594) to obtain a yield of 12077 events<sup>4</sup>. When comparing this to our side-band subtraction value from section 3 of 12010, it can be seen that they are in close agreement, although this could be further considered if the parameter error on F was determined.

Using our results from the minimisation engine, the mass value for our  $B^\pm$  mesons can be considered to be **5279.31(898)  $MeV/c^2$** . Comparing this result with the literature value ascertained from the Particle Data Group for  $B^\pm$  of 5279.34(12)  $MeV/c^2$ , it is evident that our fit is accurate, but significantly more imprecise than the Particle Data group values for  $B^\pm$ . While in the previous paragraph, it was mentioned that the  $\mu$  parameter error value was too small to be considered important, these results show that our  $\sigma$  value is oversized when compared to the literature results, as our value is well within  $1\sigma$  of the literature value. Despite this, the parameter error is still undersized, as if it was used as the error, our result wouldn't fall within  $3\sigma$  of our literature value, but would fall within  $1\sigma$  if the literature uncertainty was used.

The maximum likelihood fit was plotted over the histogram of our data, and the residuals of these differing plots were found:

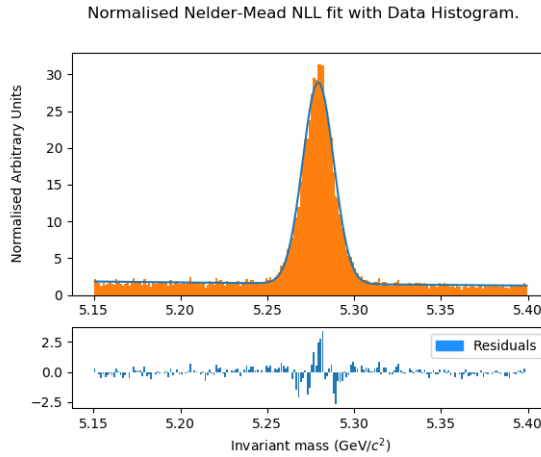


Figure 6: Normalised Fit of the Composite PDF on the initial histogram data of the mass of  $B^\pm$ , with residuals of the PDF and the histogram.

The most obvious issue with this fit is the bin height being significantly larger than the fit peak,

<sup>4</sup>Rounded down, as I believe it is inappropriate to round up and 'create' events that didn't definitively occur.

and the opposite issue along the both sides of the Gaussian distribution, which is evident in our large residual values within the Gaussian shape. This can be explained as being caused by the limited resolution of the bins being inaccurate representing the data, as our fit was found using our **unbinned** data, and so does not have the pitfalls that come with using discrete histogram data. Despite this, the difference is still quite large, and should be considered more carefully in future analysis.

## 5 Splitting $B^+$ and $B^-$ data

As can be seen in Figure 4, there is an almost equal distribution of particles with the charges  $\pm 1$ . These can be separated to either  $B^+$  or  $B^-$  mesons, and as such can be analysed separately. Using the code from the previous sections, but modifying it to apply to two different sets of data, we can obtain the results that were previously shown as  $B^\pm$ , but for each meson separately.

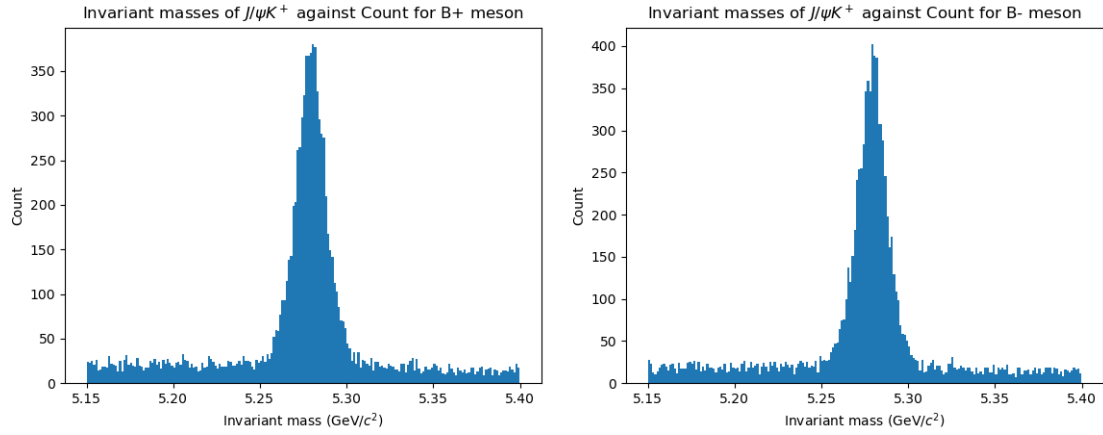


Figure 7: Distributions for  $B^+$  and  $B^-$  Mesons.

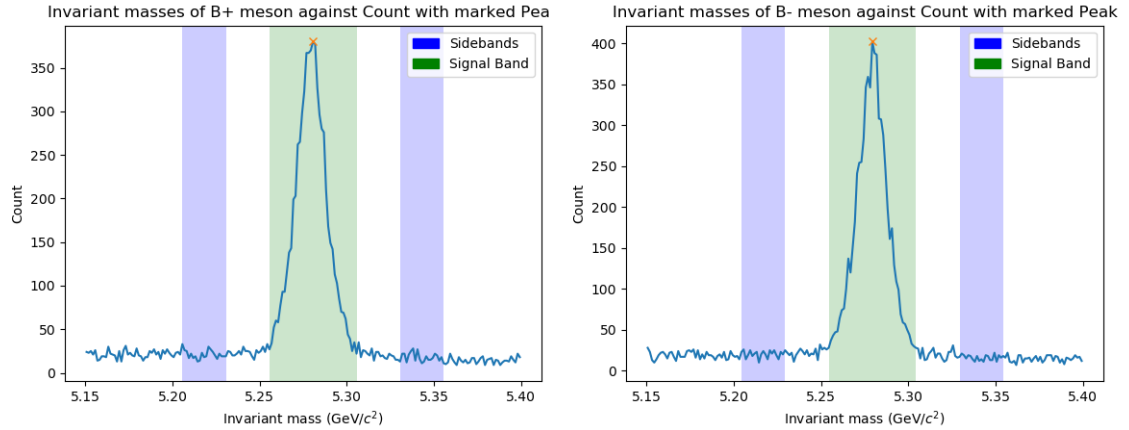


Figure 8: Side-bands for  $B^+$  and  $B^-$  Mesons, as well as the marked peaks (X).



	$B^\pm$	$B^+$	$B^-$
Estimate Peak Value ( $GeV/c^2$ )	5.279355	5.280605	5.279251
Reduced Yield Values*	12010	6013	5996
F	0.614	0.610	0.623
$\lambda$	1.446012	1.655136	1.226529
$\sigma$ ( $GeV/c^2$ )	0.00898	0.00906	0.00889
$\mu$ ( $GeV/c^2$ )	5.279305	5.279437	5.279174
$\mu$ Covariance ( $GeV/c^2$ )	9.5e-05	1.36e-04	1.33e-04

Table 1:

Table of all relevant data collected from Maximum Likelihood Fitting and Covariance calculation, as well as the estimated peak value from section 2. \*Reduced via sideband subtraction as used in section 3

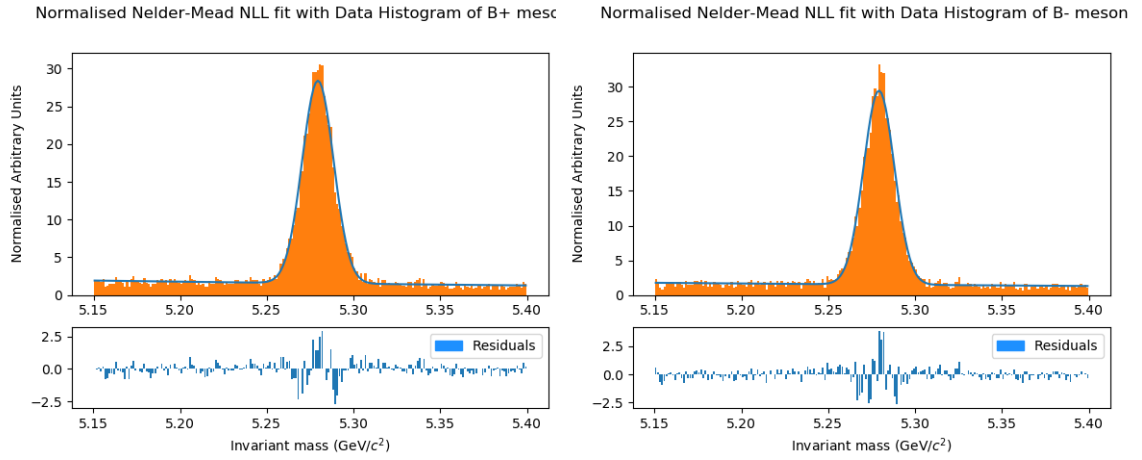


Figure 9: Normalised Fit of the Composite PDF on the initial histogram data of the mass of  $B^+$  &  $B^-$ , with residuals of the PDF and the histogram.

From this, we can take the results of the separate  $B^+$  &  $B^-$  mesons to be **5279.44(906) & 5279.17(889)  $MeV/c^2$** , with yields of **6058 & 6019** events when using the F value method, or **6013 & 5996** when using side-band subtraction. Due to the  $B^-$  meson being an antiparticle of  $B^+$ , you'd expect their masses to be identical. There are issues with this postulate in the case of our data, due to the number of events not being equal for both  $B^+$  &  $B^-$ , possibly due to the different decay modes slightly favouring other  $B^+$  meson decays. The fit is also not perfect, and the binning is once again very inaccurate at the peaks, as shown by the residuals. In spite of these glaring issues, the values for each meson are within 1  $\sigma$  of one another, regardless of which  $\sigma$  value you use (discounting the covariance values). Another factor that legitimises our results is the fact that, upon taking the average of the two mean masses, the  $B^\pm$  result of 5279.305  $MeV/c^2$  is given. This shows that our results for  $B^+$  &  $B^-$  are at the very least consistent with those of our  $B^\pm$  fitting.

## 6 Lifetime of $B^\pm$

An optional component of the project was to investigate the lifetime of the  $B^\pm$  Mesons, which is given as part of our initial data, shown in Figure 3b. It appears to be evident from the graph that the probability distribution will be exponential:

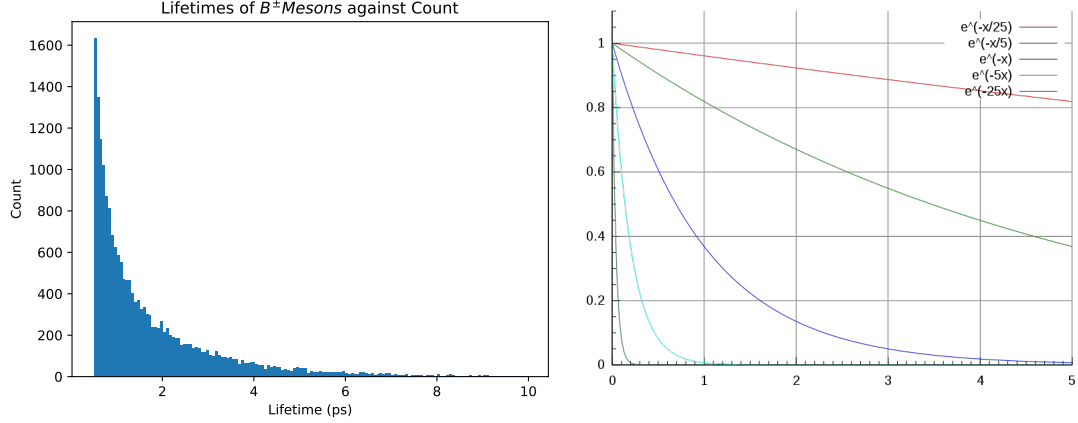


Figure 10:  $B^\pm$  lifetime with a graph of different exponential distributions [9]

From this assumption, two methods for finding the mean lifetime were used. The first being the sample mean method, which is in agreement with the negative log likelihood as derived from lecture 3 [10]. The second method is to use the fitting methods from section 4, with the PDF being altered to include only the exponent, while still calculating the variance in  $\lambda$  but ignoring the residuals<sup>5</sup>.

### 6.1 Sample Mean methods

The sample mean and variance are described as such;

$$\tau = \frac{1}{\lambda} = \frac{1}{N} \sum_{i=1}^N t_i \quad (4)$$

$$\sigma = \frac{1}{\lambda^2} \quad (5)$$

These are easily calculated within our python code for our data values, and were found to be 1.733 & 0.333 ps, giving a final value of **1.733(333)** ps. When compared to the literature value from the particle data group [6] of 1.638(4) ps, we can see that our value is larger than expected, but falls within  $1\sigma$  of the literature value. An important point is that our uncertainty is very large when compared to the literature uncertainty. This demonstrates a lack of precision in this method.

<sup>5</sup>The reasoning for this will become evident in Figure 11a

## 6.2 Maximum Likelihood Fitting methods

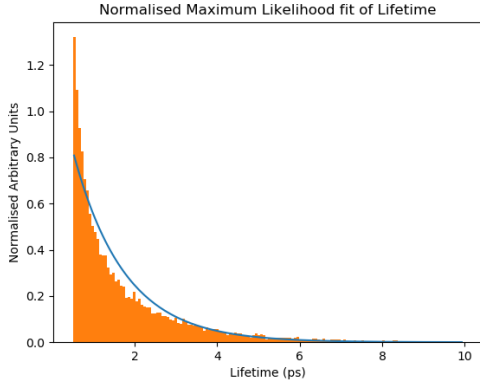
There were a lot of problems in applying the same python fitting method as used earlier for this exponential distribution. To start, two differing PDFs were tested;

$$PDF_{norm} = \frac{\lambda}{e^{-t_{min}} - e^{-t_{max}}} \cdot e^{-\lambda t} \quad (6)$$

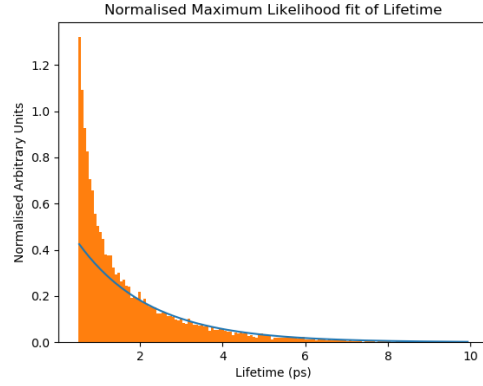
$$PDF_{standard} = \lambda \cdot e^{-\lambda t} \quad (7)$$

The former PDF derives the result normalised over our time range, from approximately 0.5 ps  $\rightarrow$  10 ps. The latter derives it with the standard range of  $0 \rightarrow \infty$ , giving the resulting normalised PDF. For both results, the lambda parameter error was calculated and used as the main error.

Equation 6 gives a  $\lambda$  value of 0.8078(58), which results in a mean lifetime value of  $\tau = \mathbf{1.2379(89)}$  ps, a result varying notably from the literature value of 1.638(4) ps [6]. The plot of this fit onto our data is also incredibly inaccurate, but could be put down to the binning used being difficult to fit near the initial time values (0.5 ps) causing the discrete histogram data to be inaccurate to the continuous PDF:



(a) Fitting using  $PDF_{norm}$



(b) Fitting using  $PDF_{standard}$

As can be seen in the figure and result, this method is not accurate or precise in terms of matching the literature value, and so the other, more standard PDF was considered. The python fitting method was kept the same, but with the new PDF, and the results gave a  $\lambda$  value of 0.5768(41), which results in a mean lifetime value of  $\tau = \mathbf{1.733(12)}$  ps. This result is in agreement with the value from section 6.1, but with a significantly lower uncertainty. While this looks promising, the lowered uncertainty now means that our value is more than  $3\sigma$  off the literature value of 1.638(4) ps. Another issue comes with the fitting, as once again the PDF fit does not match the binned data, and is in fact even more inaccurate than the previous PDF, shown in figure 11b. These figures make it evident as to why residuals are unnecessary, as it is clear by eye that the fits are inaccurate.

There are many possible reasons behind these fitting discrepancies, from the bins not appropriately representing the PDF of the data, to the possibility of the utilised PDFs not being appropriate for the data given. These factors, if given more time, would be well worth investigating, and will be touched upon in the evaluation.

## 7 Conclusion

Our total yield of our  $B^\pm$  meson in our invariant mass distribution was found to be **12078**, with a yield for  $B^+$  &  $B^-$  of **6058** & **6019** respectively. These values are in close agreement with the side-band subtraction method used earlier, but beyond this point it is very difficult to validate our results, as finding a literature value for the yield of this data was not possible. Further discussion of improvements in this area will come in the evaluation.

Our mass results for the  $B^\pm$  mesons were found to be **5279.31(898)**  $MeV/c^2$ , which is in reasonable agreement when compared to the literature value, well within  $1\sigma$  of 5279.34(12)  $MeV/c^2$ . Our uncertainty is significantly overestimated, but upon using the uncertainty provided by the literature value, our result is still within  $1\sigma$ , which demonstrates our result to be accurate, if not necessarily precise. The  $B^+$  &  $B^-$  mass results came to be **5279.44(906)** & **5279.17(889)**  $MeV/c^2$  respectively, and are within 1 and 2  $\sigma$  of the literature value, if the literature error is used. Once again our error is ignored, as it is either too large (as shown above) or too small (as seen in section 4) to be considered particularly useful in verifying our results.

Our lifetime results for  $B^\pm$  were rather inconclusive, with the result best in agreement with the literature value being taken from the sample mean method, with a value of **1.733(12)** ps. This result is still more than  $3\sigma$  from our literature value of 1.638(4) ps, and demonstrates that there are significant issues in our methodology for finding the lifetime.

## 8 Evaluation

There are lots of possible avenues for discussion when it comes to developing the veracity of this report. Hopefully in this section the most glaring of issues and possible improvements will be covered.

### 8.1 Yield results, and side-band subtraction

While results for our  $B^\pm$  mass yields are in agreement across our different methods, they cannot be claimed to be definitive. For example, the side-band subtraction method used in section 3 offers no obvious errors on our results, and only works if the number of background events are linear with changing mass. While the background events can be perceived to be linear, the use of an exponential PDF to account for them in section 4 demonstrates that this isn't so. Our side-band subtraction relies on the assumption that our exponential tail is long enough so that it can be considered to be linear. A solution for the lack of errors, but not for the linear assumption, is to use the linear least squares fitting method, which (in python) would allow us to determine covariance, and consequently errors of our yield values.

### 8.2 Parameter errors

An issue not explicitly stated in the previous section is the lack of parameter errors on a lot of values. For example, if the parameter errors for F were calculated, the maximum likelihood fitting method for finding the number of events would have given an appropriate result with errors that would have accounted for the possible non-linear nature of the background events. While the limitations of this was due to a lack of time, a possible solution (other than manually calculating the errors) would be to switch minimising engines to Minuit [11], which has been reported to not have the same issues with finding errors as SciPy's minimise engine.

Another important point to consider in the parameter errors that were calculated, is that due to the computational manner in which they were determined, they have another inherent uncertainty based on the increments taken within our error finding program. This can be minimised by decreasing the size of the increments, but it cannot be entirely removed with this method. This gives another convincing reason to swap to Minuit, as the errors calculated use a much more robust computational method when determining these errors.

### 8.3 Unbinned & binned data fitting

A point I had not considered in enough depth, was the importance of normalising our maximum likelihood fit in terms of either binned or unbinned data. The difference between the discrete distribution (as seen via our histograms) and the continuous distribution is not insignificant, and can be seen to cause issues when trying to fit one against the other<sup>6</sup>. The resolution of binned data is a large reason for the residuals found in the earlier figures (6, & 9). While this is true, increasing the resolution may not inherently improve the results, as the Gaussian trend could be washed out by noise as shown here:

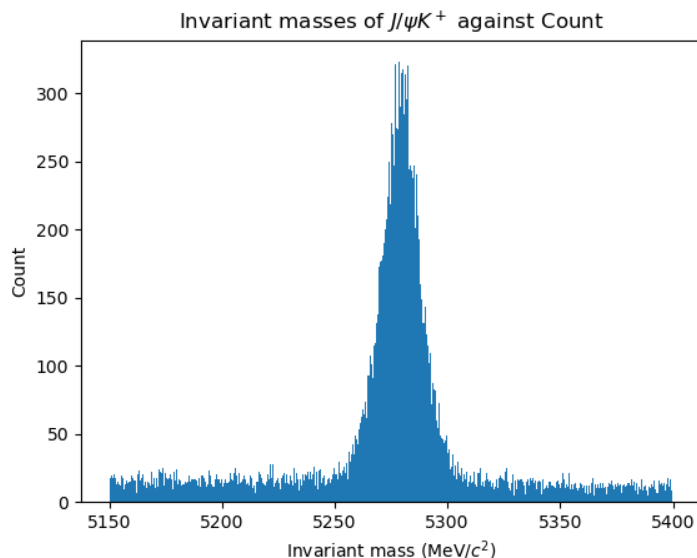


Figure 12: A graph showing the  $B^\pm$  distribution, but with 500 bins.

In this graph, it is incredible difficult to interpret the peak, as the bins are too thin and divided for any general trend to be easily ascertained. It is an important balancing act when trying to ensure a good resolution without washing out the trends that more time could have been into to choose a more optimal bin count.

### 8.4 Crystal ball fitting

It can be assumed that a Gaussian-Exponential fit is not the most optimal choice for our data. This is not only backed up by our evidently large residuals, but also by the paper this data is

---

<sup>6</sup>see figure 6

sourced from, which states that '*The  $M(J/\psi K^\pm)$  distribution is described by a probability density function (PDF) consisting of the following three components: a modified Crystal Ball (CB) function to model the signal, an exponential function to model the combinatorial background, and a double CB function to model the contamination from the Cabibbo suppressed decay  $B^\pm \rightarrow J/\psi \pi^\pm$ .*' [6]. It is evident from this that a more complex PDF was needed to accurately fit the data given. If this had been noted earlier when the code was being written, creating a crystal ball-exponential composite PDF would have been much higher up on the priority list, but due to a lack of time (and proper reading), this opportunity to better understand our data was lost.

## 8.5 The $B^+$ , $B^-$ Event discrepancy

The number of events for the  $B^+$  &  $B^-$  mass distributions were surprisingly different. This could be seen as early as figure 4, in which one of the two bins can be seen to be larger than the other. If more time was given, this could have been analysed more thoroughly to understand why this occurs in our data. It is possible that to justify this, a more comprehensive understanding of particle physics is required.

## 8.6 Lifetime Fitting

It is evident from the results of section 6 that the analysis done was not comprehensive enough to acquire any valid results beyond the sample mean method. The reasoning behind this is quite difficult to ascertain, but it is most likely due to the very small number of bins at the initial times (0.5 ps) making the PDF appear to be significantly more ill fit than is the case. This justification is quite flimsy, and doesn't hold up in the slightest when it comes to the sample mean PDF fitting. To better develop this section of the project, a lot more time would need to be invested in better understanding it. A possible solution would be to try and minimise the PDF relating to the binned data, as mentioned section 8.3, but this remains untested due to time limitations.

# 9 Acknowledgements

I would like to thank the TA's for assisting me throughout the course, as well as Dr Needham and Dr Wynne for their assistance in the coding section of the project, as I faced many issues I most likely would not have overcome without their guidance.

## 10 Bibliography

### References

- [1] The LHCb collaboration, 2017.  
Measurement of the  $B^\pm$  production cross-section in pp collisions at  $\sqrt{s} = 7$  and 13 TeV.  
J. High Energ. Phys. 2017, 26.  
[https://doi.org/10.1007/JHEP12\(2017\)026](https://doi.org/10.1007/JHEP12(2017)026)
- [2] The LHCb Collaboration, 2009.  
Roadmap for selected key measurements of LHCb.  
arXiv:0912.4179 [hep-ex].
- [3] Niel, E.M., Bruno, G.E., Betev, L., 2017  
FONLL calculations for heavy quark production in nuclear collisions.  
<https://cds.cern.ch/record/2282263>
- [4] CDF Collaboration, 2006.  
Observation of  $B_s^0 \rightarrow \psi(2S)\phi$  and measurement of the ratio of branching fractions  $\mathbf{B}(B_s^0 \rightarrow \psi(2S)\phi)/\mathbf{B}(B_s^0 \rightarrow J/\psi\phi)$ .  
Physics Research Publications 96.
- [5] find\_peaks documentation - SciPy  
[https://docs.scipy.org/doc/scipy/reference/generated/scipy.signal.find\\_peaks.html](https://docs.scipy.org/doc/scipy/reference/generated/scipy.signal.find_peaks.html)
- [6] P.A. Zyla et al. (Particle Data Group) 2020.  
083C01 (2020),  $B^\pm$  Particle Listing  
Prog. Theor. Exp. Phys.
- [7] curve\_fit documentation - SciPy  
[https://docs.scipy.org/doc/scipy/reference/generated/scipy.optimize.curve\\_fit.html](https://docs.scipy.org/doc/scipy/reference/generated/scipy.optimize.curve_fit.html)
- [8] scipy.optimize.minimize - SciPy  
<https://docs.scipy.org/doc/scipy/reference/generated/scipy.optimize.minimize.html>
- [9] Autopilot, P. png: P. work:, 2010.  
English: This diagram shows exponential decay in a graphical form.  
Wikimedia Commons  
<https://commons.wikimedia.org/wiki/File:Plot-exponential-decay.svg>
- [10] Matthew Needham, Ben Wynne  
Data Acquisition and Handling - Lecture 3, Fitting  
University of Edinburgh, School of Physics & Astronomy
- [11] CERN - Fred James, Matthias Winkler, 2014.  
<https://root.cern.ch/root/html/doc/guides/minuit2/Minuit2.html>